Structure of a Nonadecapeptide of the Fifth EGF Domain of Thrombomodulin Complexed with Thrombin[†,‡]

I. I. Mathews, K. P. Padmanabhan, and A. Tulinsky*

Department of Chemistry, Michigan State University, East Lansing, Michigan 48824-1322

J. Evan Sadler

Howard Hughes Medical Institute, Departments of Medicine and Biochemistry and Molecular Biophysics, The Jewish Hospital of St. Louis, Washington University School of Medicine, St. Louis, Missouri 63110

Received August 12, 1994; Revised Manuscript Received September 26, 1994[⊗]

ABSTRACT: The crystallographic structure has been determined of a complex between a nonadecapeptide from the fifth epidermal growth factor (EGF5) domain of human thrombomodulin and human D-PheProArg-α-thrombin. The peptide corresponds to amino acid residues Glu408−Glu426 of thrombomodulin and contains the third disulfide loop of EGF5 and its linker to EGF6. The structure was refined at 3.0-Å resolution to an *R*-value of 0.146. There are two thrombin molecules in the asymmetric unit, and the structure in the crystal is a 2:1 thrombin complex. The folding of the peptide corresponds closely to the third disulfide loop of EGF2 of factor Xa (rmsΔ = 1.0 Å). The peptide is squeezed between cofacial electropositive fibrinogen recognition exo sites of the two thrombin molecules. Since the peptide has a total of seven aspartic and glutamic acid residues, the principal binding interaction with thrombin is electrostatic. A major hydrophobic association, which is highly directional in such a pronounced electrostatic environment, involves a TyrIleLeu triplet of the peptide and Phe34, Leu65, Tyr76, and Ile82 (chymotrypsinogen numbering) of one thrombin molecule. The tyrosine of the peptide is sandwiched between the thrombin aromatic rings and is most likely the prime source of the specificity of the thrombomodulin−thrombin interaction.

Two distinct anticoagulant mechanisms are triggered by contact with cell surfaces. One involves surface heparin-like molecules that function to accelerate the inactivation of coagulation proteases by antithrombin III (Rosenberg & Rosenberg, 1984). The other involves thrombomodulin, a thrombin-binding cell surface receptor that alters the macromolecular specificity of thrombin by decreasing its ability to catalyze clot formation while at the same time converting thrombin into a potent protein C activator (Esmon & Owen, 1981; Esmon, 1989). Activated protein C functions as an anticoagulant by inactivating factors Va and VIIIa (Nesheim et al., 1982), two regulatory proteins of the coagulation pathway that participate in the activation of factors X and IX, respectively. Formation of the thrombin−thrombomodulin complex directly curtails the capacity of thrombin to convert fibrinogen to fibrin and to activate blood platelets (Esmon et al., 1983; Suzuki et al., 1986; Hofsteenge et al., 1986).

Thrombomodulin is a high-affinity receptor of thrombin forming a 1:1 complex with a $K_d = 0.5$ nM (Esmon & Owen, 1981). Thrombomodulin contains 559 residues and consists of five domains. The N-terminal domain has limited similarity to lectin-like molecules and is followed by six modules that are homologous to EGF[1] repeats. The extracellular region is completed with a much smaller segment rich in O-linked carbohydrates. This is followed by a membrane spanning domain and a short cytoplasmic domain (Wen et al., 1987). The fragments consisting of EGF1−6 (Kurosawa et al., 1987) and EGF4−6 (Hayashi et al., 1990) interact with both protein C and thrombin and retain cofactor activity while EGF5−6 lacks cofactor activity but retains a high-affinity thrombin binding site (Stearns et al., 1989; Tsiang et al., 1992).

The synthetic peptide ECPEGYILDDGFICTDIDE, corresponding to Glu408−Cys421 of EGF5 (C-terminal disulfide loop) and the Thr422−Glu426 linker between EGF5 and EGF6 (Figure 1), inhibits thrombin binding to thrombomodulin with a K_i of 95 nM (Hayashi et al., 1990; Tsiang et al., 1990). Alanine-scanning mutagenesis of EGF4−6 further indicates that Glu408, YILDD, and DIDE of the nonadecapeptide sequence are critical for thrombin binding (Nagashima et al., 1993). We report here the X-ray crystal structure determination of the complex between the 19-residue peptide bound in the fibrinogen recognition exo site of PPACK-inhibited α-thrombin and describe the general and specific nature of the interactions involved in the exo site, which are also most likely operative in the thrombomodulin−thrombin complex.

[†] This work was supported by NIH Grants HL43229 (A.T.) and HL14147 (J.E.S.).

[‡] Coordinates of the asymmetric unit have been deposited in the Brookhaven Protein Data Bank, Accession Number 1HLT.

* To whom correspondence should be addressed: telephone 517-355-9715 X250; FAX 517-353-1793.

[⊗] Abstract published in *Advance ACS Abstracts,* November 1, 1994.

[1] Abbreviations: EGF, epidermal growth factor; PPACK, D-Phe-ProArg chloromethyl ketone; hirugen, sulfatoTyr63-hirudin53−64; MALDI-MS, matrix-assisted laser desorption ionization mass spectrometry; PHMB, *p*-(hydroxymercuri)benzoate; TCEP, tris(2-carboxyethyl)phosphine.

0006-2960/94/0433-13547$04.50/0

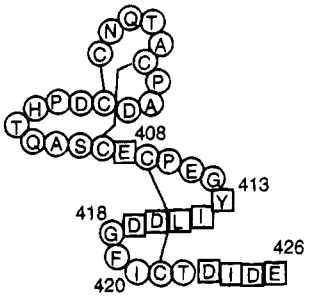

FIGURE 1: Sequence of EGF5 of thrombomodulin and linker to EGF6. The 19-residue peptide in the present work is Glu408–Glu426; residues in squares are implicated in thrombin binding by alanine-scanning mutagenesis (Nagashima et al., 1993).

EXPERIMENTAL PROCEDURES

Thrombomodulin 408–426 was synthesized with an ABI Model 430 peptide synthesizer using *tert*-butyloxycarbonyl chemistry and standard cycle conditions and purified by reverse-phase HPLC (Tsiang et al., 1992). The peptide was ~92% pure as assessed by analytical reverse-phase HPLC. The amino acid composition and sequence by automated Edman degradation agreed with expectation.

PPACK–thrombin was used to prepare the complex to ensure against autolysis of thrombin. Human α-thrombin was supplied by Dr. John W. Fenton II as frozen samples at a concentration of 0.81 mg/mL in 0.75 M NaCl. The PPACK–thrombin was made by placing a 10-fold molar excess of solid chloromethyl ketone on the frozen thrombin sample that was allowed to thaw. The resulting solution was diluted with an equal amount of 0.1 M sodium phosphate buffer (pH 7.3) and concentrated to 3.8 mg/mL using Centricon-10 miniconcentrators in a refrigerated centrifuge. A 10-fold molar excess of the thrombomodulin peptide was then added to the concentrated PPACK–thrombin. Two types of crystals (bipyramidal and square plates) were obtained from hanging drops made of 4 μL of ternary protein complex with 4 μL of reservoir solution. The reservoir solution consisted of 26% PEG 8000, 0.1 M sodium phosphate buffer (pH 7.3), and 1 mM NaN_3. Although the bipyramidal-shaped crystals were larger, they only diffracted X-rays poorly (3.8-Å resolution). Square plates of 0.4 × 0.4 × 0.05 mm in size were better, diffracting to 3.0-Å resolution, and were used for intensity data collection.

Intensities were measured with a R-AXIS imaging plate detector and graphite monochromated Cu Kα radiation from a Rigaku RU200 rotating anode generator. The square plate crystals are tetragonal with an unusually elongated unit cell of $a = b = 50.88$ Å and $c = 325.8$ Å (c-axis perpendicular to the flat face) with space group $P4_1$ ($P4_3$). There are eight thrombin molecules in the unit cell (two per asymmetric unit, 45% protein fraction, $V_m = 2.75$ Å/Da). The intensity data were collected from two crystals in different mounting positions. The crystal to detector distance was 275 mm for both, and air absorption was reduced using a helium accordion between the crystal and the detector. To utilize the pixel resolution of the imaging plate to advantage and circumvent very small oscillation angles that might possibly be associated with the long axis, the first data set was collected with the a–c plane perpendicular to the beam (a-axis parallel to the spindle of the detector) at a detector swing angle of 10.5° (23 frames, 12 048 unique reflections, 69% $|F|^2 > 1\sigma$, $R_{merge} = 0.068$), while the c-axis was oriented parallel to the spindle axis for the second set (7 frames, 5020 unique reflections, 30% $|F|^2 > 1\sigma$, $R_{merge} = 0.038$). In the latter orientation, the flat face of the crystal was supported by a column of rolled mylar film. The two sets were scaled and averaged, rejecting reflections with $2(|F_1|^2 - |F_2|^2)/(|F_1|^2 + |F_2|^2) > 0.40$. This gave a data set of 12 757 reflections (77%) at 3.0-Å resolution with an R-value of 0.090 between common reflections of the two independent sets.

The structure of the complex was solved by molecular replacement rotation/translation methods. A self-rotation function was calculated using the program X-PLOR (Brunger, 1990) to fix the noncrystallographic symmetry relating the independent thrombin molecules. The highest peak was 4.2σ above the mean, and the angles corresponded to a noncrystallographic 2-fold rotation approximately parallel to the b-axis. The thrombin coordinates of the hirugen–thrombin complex (Skrzypczak-Jankun et al., 1991) were used as the model in a cross-rotation search. The two highest solutions had peak heights 3.5σ and 3.2σ above the mean, and the rotation matrices of the individual molecules were in agreement with the self-rotation matrix. Translation searches were performed in both enantiomorphic space groups with $P4_3$ giving better results. The search was initially conducted using individual molecules in the xy plane (correlation coefficients of 0.37 and 0.39, with peak heights 11.3σ and 12.1σ above the mean). The two molecules belonging to the same asymmetric unit were selected by displaying the results with graphics, which also showed that the fibrinogen recognition exo sites were cofacial and close to the local 2-fold axis. A rigid body refinement with both molecules together gave an R-value of 0.35 in the 8.0–4.0-Å resolution range.

The starting dimer structure was refined using restrained least-squares methods employing the program PROFFT (Finzel, 1987). After 21 cycles, the refinement converged to a crystallographic R-value of 0.233. The electron and difference density maps clearly indicated the presence of PPACK in the active site and two strands of electron density in the fibrinogen recognition exo site corresponding to the thrombomodulin peptide. The electron density of the thrombomodulin peptide was squeezed in between the thrombin molecules at right angles to the local symmetry axis. Since the density of the peptide additionally showed poor local symmetry and there were no indications of another peptide in the asymmetric unit, all the foregoing clearly suggested that the latter consisted of two thrombin molecules and one thrombomodulin peptide in a 2:1 complex. Further refinement proceeded including nine alanine residues in calculations, without symmetry, corresponding to the thrombomodulin peptide but applying noncrystallographic symmetry restraints to the PPACK–thrombin molecules. Solvent was included in the model as water molecules at $R = 0.185$ that improved the density of some of the side chains of the peptide and revealed an additional smaller strand near the thrombomodulin peptide. A completely satisfactory interpretation of the thrombomodulin peptide electron density was achieved in a comparative study of the density-fitted peptide residues and the folding of EGF2 of factor Xa (Padmanabhan et al., 1993a): the three-strand region of the C-terminal disulfide loop of EGF2 of factor Xa and some of its connecting linker to the catalytic domain corresponded closely to the backbone of the thrombomodulin peptide. Most of the side chains of the thrombomodulin peptide could then

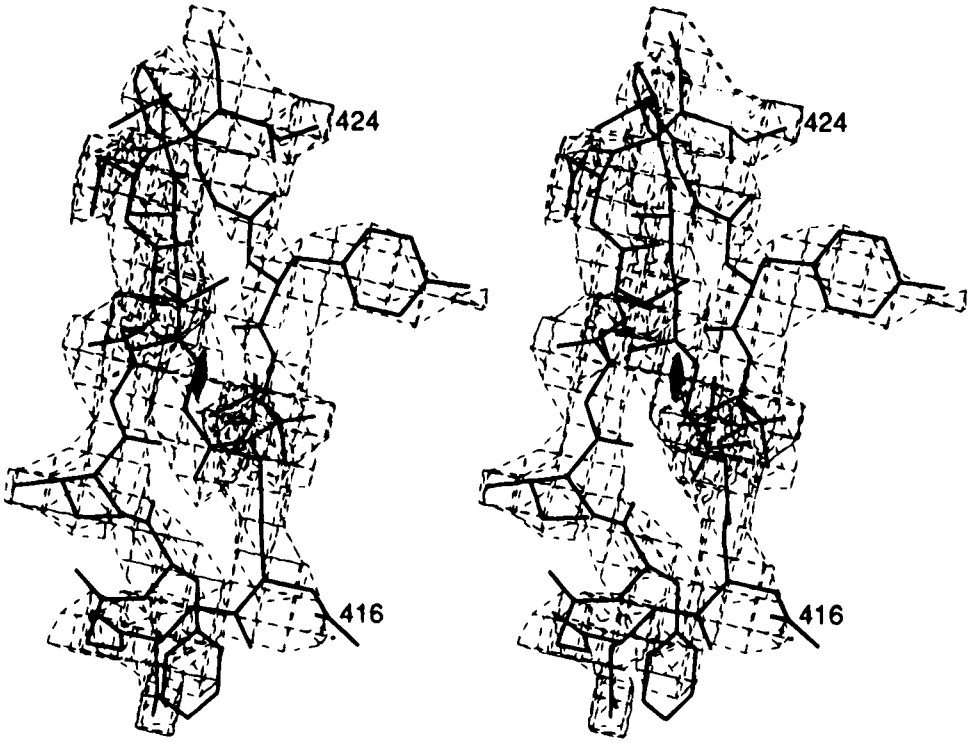

FIGURE 2: Stereoview of the final $(2|F_o| - |F_c|)$ electron density of the thrombomodulin peptide viewed along the local 2-fold rotation axis. No density is present at Glu411 and Asp425Glu426. Contoured at the 1σ level. The local 2-fold axis is shown appropriately.

be modeled, and further refinement proceeded smoothly to $R = 0.146$. The average thermal parameter of the 2:1 complex containing 121 water molecules is 23 Å. The rms differences from ideal bond and bond angle lengths are 0.012 and 0.048 Å, respectively. The coordinates of the asymmetric unit have been deposited in the Brookhaven Protein Data Bank.

RESULTS AND DISCUSSION

When thrombin interacts with thrombomodulin, it undergoes a conformational change that alters the substrate specificity of thrombin by increasing its rate of activation of protein C about 20 000-fold, which also regulates blood coagulation (Esmon et al., 1983; Ye et al., 1991). Chemical modifications of the active site His57 and Ser195 (chymotrypsinogen numbering; Bode et al., 1992) residues and deglycosylation of thrombin do not alter interactions with thrombomodulin, but modification of arginine, tryptophan, or tyrosine residues can cause a loss in affinity (Thompson & Salem, 1988). β-Thrombin and γ-thrombin have reduced abilities to activate protein C (Fenton, 1986), and γ-thrombin does not displace α-thrombin from thrombomodulin (Bezeaud et al., 1985). Single amino acid substitution studies have shown that thrombin with anticoagulant activity can be created by mutagenesis (Lys60F → Glu); in addition, the thrombomodulin binding site overlaps the fibrinogen recognition exo site, but the two are not identical (Wu et al., 1991).

The electron density of most of the Glu408−Glu426 thrombomodulin peptide is well-defined except for Glu411 at a sharp reverse turn and the last two residues (Asp425−Glu426) (Figure 2). Although the peptide is at right angles to and near the local 2-fold axis relating the independent thrombin molecules of the asymmetric unit, the electron density of the peptide does not correspond to a symmetry-averaged structure but rather to that of a single molecular entity. Therefore, the stoichiometry of the thrombin−thrombomodulin peptide complex is 2:1 in the crystal structure.

The folding of the thrombomodulin peptide corresponds closely to that of the third disulfide loop of the second EGF domain of factor Xa (Padmanabhan et al., 1993a). The rms difference in main-chain positions for 16 of the residues is 1.0 Å (Figure 3). The peptide between the cysteines and its accompanying inter-EGF linker is in a three-strand antiparallel β-sheet conformation (Glu408−Pro410, Gly412−Asp416, Phe419−Asp423) with hydrogen bonds between Tyr413O−Thr422N, 2.5 Å, Leu415N−Ile420O, 2.7 Å, and possibly Glu408N−Cys421S, 3.1 Å. The folding also corresponds to that of the comparable disulfide loops of other EGF domains of known three-dimensional structure (Campbell et al., 1989; Padmanabhan et al., 1993a).

Although the electron density of the sulfur atom of Cys421 of the thrombomodulin peptide is well-defined, that of Cys409 is not. This, coupled with the overall resistance of the peptide to air oxidation (D. Nitechi, Berlex Biosciences, personal communication), suggested that the peptide may be in a reduced oxidation state in the complex and led to the characterization of the peptide by MALDI-MS. Four experiments were carried out: spectra were measured of the peptide with and without PHMB present, and these were repeated, but first treating the peptide with the reducing agent TCEP. The two pairs of spectra were the same, indicating molecular masses of 2148.2 Da for a reduced thrombomodulin peptide and 2468.6 and 2789.5 Da corresponding to the reduced mono- and disubstituted PHMB derivatives (molecular mass of PHMB = 321 Da). The original peptide material, therefore, is in a reduced oxidation state and most likely remains so in the crystalline complex. When the first cysteine of the thrombomodulin peptide is changed to alanine, the linear peptide competes with thrombomodulin

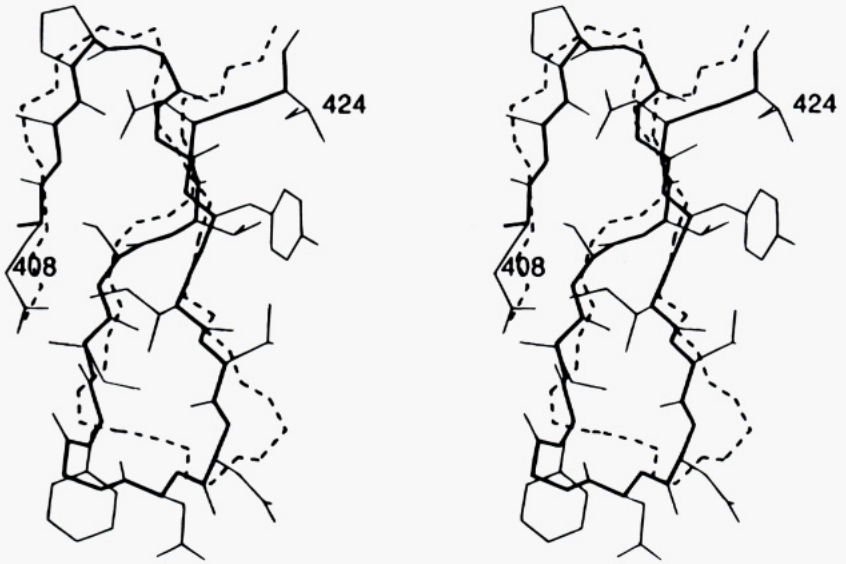

FIGURE 3: Stereoview comparing the folding of the thrombomodulin peptide (bold) with that of the disulfide loop of EGF2 of factor Xa (dotted). Side groups of the thrombomodulin peptide are also shown.

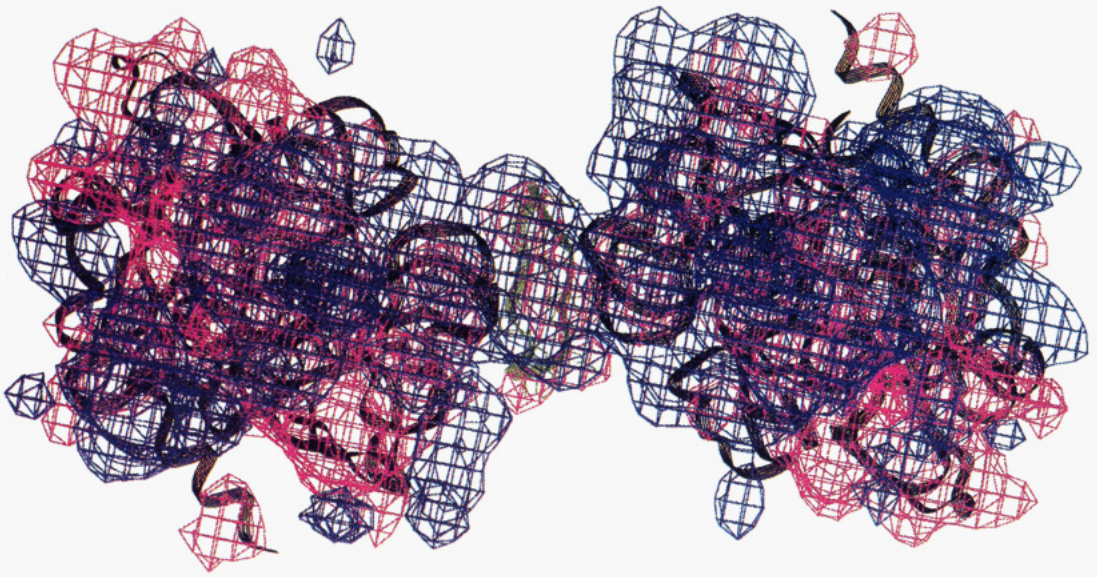

FIGURE 4: Electrostatic potential of the 2:1 thrombin−thrombomodulin peptide complex. Viewed along the local 2-fold axis; contours at 3 kT; blue, positive; red, negative; thrombin ribbon, black; thrombomodulin peptide ribbon, green; calculated with DELPHI of the Biosymm Suite using 0.15 for the ionic strength of the solvent.

for thrombin binding with an affinity similar to that of the cysteine peptide (Tsiang et al., 1992). It is noteworthy that the reduced peptide folds into the same structure as the oxidized disulfide loop found in intact EGF domains, suggesting that the sequence or the thrombin interaction dictates the folding of the region. The latter is not inconsistent with the same structure being found in the second EGF of factor Xa and isolated EGF domains (Padmanabhan et al., 1993a) if the interaction of the third and first two loops of an EGF module also fold the third loop.

The structures of the two independent thrombin molecules of the complex are practically the same at 3.0-Å resolution (rmsΔ = 0.47 Å, main chain; 0.8 Å, side chains) and are very similar to those of hirugen−thrombin and PPACK−thrombin. The fibrinogen recognition exo sites of the two thrombin molecules of the complex are cofacial to one another and close to the local 2-fold rotation axis. The fibrinogen binding exo site is highly electropositive (Karshikov et al., 1992) so the region of the local 2-fold axis at the thrombomodulin peptide between thrombin molecules is much more electropositive. However, the peptide contains eight carboxylate groups counting the C-terminal[2] that compensate some of the charge and reduce the electrostatic potential, but the region still remains electropositive (Figure 4). To a first approximation then, thrombin must be electrostatically attracted to the third loop of the fifth EGF module of thrombomodulin and its linker to EGF6. A somewhat similar electrostatic interaction occurs in crystals between the negatively charged GGTTGGTGTGGTTGG single-stranded DNA aptamer and two thrombin molecules, except that the electropositive heparin binding site of one of the thrombin molecules is involved in concert with the fibrinogen recognition site of the other (Padmanabhan et al., 1993b).

Since the stoichiometry of the complex is 2:1 thrombin−peptide in the crystal, two possible binding modes are

[2] The excessive negative charge may be related to the resistance of the cysteines to oxidation.

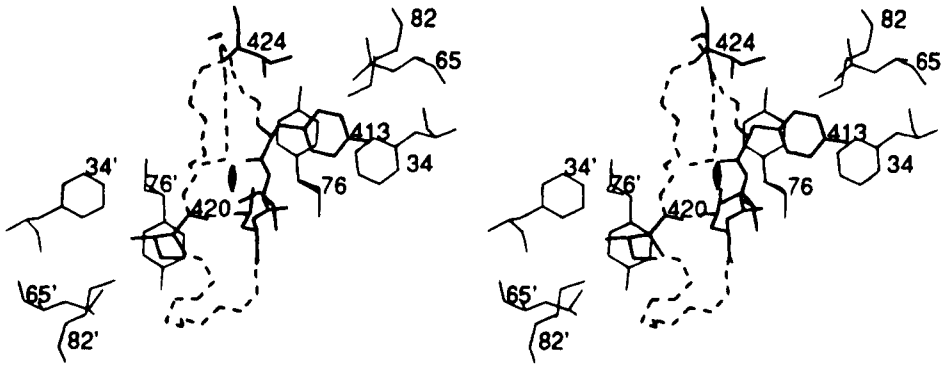

FIGURE 5: Stereoview of hydrophobic interactions of the thrombomodulin peptide between two thrombin molecules viewed along the local 2-fold rotation axis. The thrombomodulin peptide backbone is dotted, interacting side chains are in bold, and thrombin is in thin lines. Prime numbers are molecule 2 in the text. The local 2-fold axis is shown appropriately.

Table 1: Thrombomodulin Peptide–Thrombin Polar Interactions[a]

peptide	thrombin	distance (Å)	comments
Tyr413OH	Arg67NE	2.4	hydrogen bond
Ile414N	Gln38OE1	2.9	hydrogen bond
Asp416OD1	Arg75NH1	3.0	H-bonded ion pair
Asp416OD1	Arg77A'NH1	3.7	ion pair
Asp416OD2	Thr74OG1	2.5	hydrogen bond
Asp417OD1	Arg77A'NH1	4.1	ion pair
Thr422OG1	Arg77ANH1	2.6	hydrogen bond
Asp423O	Arg75'NH1	3.1	hydrogen bond

[a] Prime notation designates molecule 2 of thrombin.

Table 2: Comparison of the Loop Lengths of the Fifth EGF of Thrombomodulin with Other EGF Domains

		loop lengths (no. of residues)		
domain	species	I	II	III
fifth EGF	human	10	13	13
second FXa EGF	human	12	14	14
first FX EGF	bovine	12	16	10
first FIX EGF	human	12	16	10
EGF	mouse/human	15	18	10
TGF[a]	human	14	17	10

[a] TGF is transforming growth factor.

revealed for the thrombomodulin peptide with the fibrinogen binding exo site (Figure 5). The major hydrophobic interactions, which should be highly directional in such a hostile electrostatic environment, occur, utilizing Tyr413–Leu415, Ile424, and Ile420. A hydrophobic patch on the thrombin surface composed of Phe34, Leu65, Tyr76, and Ile82 shelters Tyr413 of the peptide from the electrostatic charge (Figure 5) making two aromatic stacking interactions with Tyr413, in agreement with alanine-scanning mutagenesis that implicated the Tyr413–Asp417 residues as determinants in thrombin binding with Ile424 → Ala showing the largest effect (Nagashima et al., 1993). The Ile414, Leu415, and Ile424 complete the hydrophobic region of the peptide (Figures 2, 3, and 5). The Ile420 residue partially occupies the same hydrophobic site, but of the other thrombin molecule (molecule 2), making three van der Waals contacts of less than 4.0 Å (Figure 5), but was not implicated by the scanning mutagenesis.

The thrombomodulin peptide hydrophobic site of thrombin is occupied by Ile59 in hirugen–thrombin (Skrzypczak-Jankun et al., 1991) and phenylanine in the hirullin (Qiu et al., 1993) and thrombin platelet receptor–peptide complexes of thrombin (Mathews et al., 1994); the chain direction of the thrombomodulin peptide, however, is opposite to the other three. Fairly specific ionic interactions also occur in the interface: Asp416 forms salt bridges with both molecules (Asp416OD1–Arg75NH1, 3.0 Å, molecule 1; Asp416OD1–Arg77ANH1, 3.7 Å, molecule 2) while Asp417 also makes an ion pair with Arg77A of molecule 2 (Table 1). The Arg77A interactions, however, appear to be more a bifurcated intermolecular ion pair between a thrombomodulin peptide–thrombin complex and a neighboring thrombin molecule in the crystal. The specific polar interactions are completed with four more hydrogen bonds with molecule 1 and another between Asp423O and Arg75NH1 of molecule 2 (Table 1).

The thrombomodulin residues of EGF5 and its linker to EGF6 that were implicated as determinants of thrombin binding by alanine-scanning mutagenesis are Glu408, Tyr413–Asp417, and Asp423–Glu426 (Figure 1) (Nagashima et al., 1993). Of these, Tyr413–Asp417, Asp423, and Ile424 (Asp425Glu426 are flexibly disordered) have close contacts with molecule 1 of the 2:1 complex,[3] so this must be the thrombomodulin–thrombin interaction site in the physiological macromolecular complex. The interactions with molecule 2 are much less extensive, involving only Asp417, Ile420, and Asp423. The Asp417 appears to be in an intermolecular crystal packing interaction and makes a single hydrogen bond with thrombin. The Ile420 was not implicated by scanning mutagenesis and happens to be fortuitously related to Tyr413Ile414Leu415 by a 2-fold axis. Although Glu411 and Asp425Glu426 are flexibly disordered, the negative charges resulting from them are likewise approximately 2-fold related to similar charges of Asp416–Asp417 at the other end of the β-strand structure of the thrombomodulin peptide. Since the surface at Ile420 of the thrombomodulin peptide in the "1:1 thrombin complex" mimics that of the primary binding site of the thrombomodulin peptide alone, a thrombin fibrinogen binding exo site of another thrombin molecule appears to be naturally attracted to it during crystallization to form the 2:1 thrombin complex that even shields Ile420 from the highly charged environment.

Of EGF modules with known three-dimensional structures (Table 2), the loop sizes of EGF5 of thrombomodulin are best approximated by EGF2 of factor Xa (Padmanabhan et al., 1993a). Moreover, it has been shown here that the

[3] Only Glu408 is not implicated by the crystallography. This may be related to the reduced disulfide bond of the peptide in crystals and the adjacent disorder of Cys409S.

ordinary simple disulfide loop of the triple loop structure of EGF2 of factor Xa and part of its linker peptide has close similarity in folding to the thrombomodulin peptide Glu408–Glu426. This led us to a more extended comparative study using the coordinates of EGF2. The main chain of Cys411–Thr427 of the complete EGF2 module was superimposed on the thrombomodulin peptide in a "1:1 EGF2 thrombin complex." The resulting model did not reveal any additional EGF contact regions of the first two disulfide loops with thrombin, in agreement with the alanine-scanning mutagenesis (Nagashima et al., 1993). However, when the EGF2 was docked to molecule 2 of thrombin (binding through Ile420), massive collisions occurred in the interface of thrombin and the remainder of the EGF2 module because Ile420 is buried in the EGF model. This indicates further that the binding interactions between thrombin and thrombomodulin must be those associated with molecule 1 of thrombin.

ACKNOWLEDGMENT

We thank Dr. Eugene Zaluzec of the Michigan State University NIH Mass Spectroscopy Facility for performing the MALDI-MS experiments, Dr. Koji Suzuki for providing us with an initial 4-mg sample of the thrombomodulin peptide, and John Gorka (HHMI Biopolymers Facility, Washington University, St. Louis, MO) for large-scale synthesis and purification of the thrombomodulin peptide.

REFERENCES

Bezeaud, A., Denninger, M.-H., & Guillin, M.-C. (1985) *Eur. J. Biochem. 153*, 491–496.

Bode, W., Turk, D., & Karshikov, A. (1992) *Protein Sci. 1*, 426–471.

Brunger, A. T. (1990) *X-PLOR Manual, Version 2.1*, Yale University, New Haven, CT.

Campbell, I. D., Cooke, R. M., Harvey, T. S., & Tappin, M. J. (1989) *Prog. Growth Factor Res. 1*, 13–22.

Esmon, C. T. (1989) *J. Biol. Chem. 264*, 4743–4746.

Esmon, C. T., & Owen, W. G. (1981) *Proc. Natl. Acad. Sci. U.S.A. 78*, 2249–2252.

Esmon, N. L., Carroll, R. C., & Esmon, C. T. (1983) *J. Biol. Chem. 258*, 12238–12242.

Fenton, J. W., II (1986) *Ann. N.Y. Acad. Sci. 485*, 5–15.

Finzel, B. C. (1987) *J. Appl. Crystallogr. 20*, 53–55.

Hayashi, T., Zushi, M., Yamamoto, S., & Suzuki, K. (1990) *J. Biol. Chem. 265*, 20156–20159.

Hofsteenge, J., Taguchi, H., & Stone, S. R. (1986) *Biochem. J. 237*, 243–251.

Karshikov, A., Bode, W., Tulinsky, A., & Stone, S. R. (1992) *Protein Sci. 1*, 727–735.

Kurosawa, S., Galvin, J. B., Esmon, N. L., & Esmon, C. T. (1987) *J. Biol. Chem. 262*, 2206–2212.

Mathews, I. I., Ganesh, V., Padmanabhan, K. P., Tulinsky, A., Ishii, M., Chen, J., Turch, C. W., & Coughlin, S. R. (1994) *Biochemistry 33*, 3266–3279.

Nagashima, M., Lundh, E., Leonard, J. C., Morser, J., & Parkinson, J. F. (1993) *J. Biol. Chem. 268*, 2888–2892.

Nesheim, M. E., Canfield, W. M., Kisiel, W., & Mann, K. G. (1982) *J. Biol. Chem. 257*, 1443–1447.

Padmanabhan, K., Padmanabhan, K. P., Tulinsky, A., Park, C. H., Bode, W., Huber, R., Blankenship, D. T., Cardin, A. D., & Kisiel, W. (1993a) *J. Mol. Biol. 232*, 947–966.

Padmanabhan, K., Padmanabhan, K. P., Ferrara, J. D., Sadler, J. E., & Tulinsky, A. (1993b) *J. Biol. Chem. 268*, 17651–17654.

Qiu, X., Yin, M., Padmanabhan, K. P., Krstenansky, J. L., & Tulinsky, A. (1993) *J. Biol. Chem. 268*, 20318–20326.

Rosenberg, R. D., & Rosenberg, J. S. (1984) *J. Clin. Invest. 74*, 1–6.

Skrzypczak-Jankun, E., Carperos, V. E., Ravichandran, K. G., Tulinsky, A., Westbrook, M., & Maraganore, J. M. (1991) *J. Mol. Biol. 221*, 1379–1393.

Stearns, D. J., Kurosawa, S., & Esmon, C. T. (1989) *J. Biol. Chem. 264*, 3352–3356.

Suzuki, K., Kusumoto, H., & Hashimoto, S. (1986) *Biochim. Biophys. Acta 882*, 343–352.

Thompson, E. A., & Salem, H. H. (1988) *Thromb. Haemostasis 59*, 415–420.

Tsiang, M., Lentz, S. R., Dittman, W. A., Wen, D., Scarpati, E. M., & Sadler, J. E. (1990) *Biochemistry 29*, 10602–10612.

Tsiang, M., Lentz, S. R., & Sadler, J. E. (1992) *J. Biol. Chem. 267*, 6164–6170.

Wen, D., Dittman, W. A., Ye, R. D., Deavan, L. L., Majerus, P. W., & Sadler, J. E. (1987) *Biochemistry 26*, 4350–4357.

Wu, Q., Sheehan, J. P., Tsiang, M., Lentz, S. R., Birktoft, J. J., & Sadler, J. E. (1991) *Proc. Natl. Acad. Sci. U.S.A. 88*, 6775–6779.

Ye, J., Esmon, N. L., Esmon, C. T., & Johnson, A. E. (1991) *J. Biol. Chem. 266*, 23016–23021.